Contrib Mineral Petrol (1993) 114:203–220

Contributions to Mineralogy and Petrology

Diffusion controlled growth of pyroxene-bearing margins on amphibolite bands in the granulite facies of Rogaland (Southwestern Norway): implications for granulite formation

J. Vander Auwera

Laboratoires associés de Géologie, Pétrologie et Géochimie, Université de Liège, B-4000 Sart Tilman, Belgium

Received January 21, 1991 / Accepted November 26, 1992

Abstract. In the Rogaland granulites of Southern Norway, thin anhydrous pyroxene-bearing margins (5–10 mm) are observed mainly in migmatitic banded gneisses at the contact between hornblende-rich metabasites and charnockites. According to field data, the development of these margins post-dates any deformation. Petrographic data show that they are zoned. Three different types have been recognized:–

1. Metabasite/plagioclase + orthopyroxene/plagioclase + clinopyroxene/gneiss
2. Metabasite/plagioclase + orthopyroxene + clinopyroxene/plagioclase + clinopyroxene/gneiss
3. Metabasite/plagioclase + orthopyroxene/gneiss

The first zone corresponds to the reaction of amphibole and biotite of the metabasite into pyroxenes. The second zone, which is not present in the third type, developed essentially at the expense of gneiss and the Z1/Z2 boundary is likely to correspond to the original contact between metabasite and gneiss. When the anorthite content of plagioclase and the Fe no. of pyroxenes are strongly different between adjacent metabasite (An_{38-40} for plagioclase; Fe no. [Fe/(Fe + Mg)], 0.51–0.52 for orthopyroxene) and gneiss (An_{22-26}; Fe no., 0.58–0.59), the solid solution compositions evolve continuously through the margin from the value in the metabasite to that in the gneiss. On the other hand, a margin is also present when plagioclase and pyroxenes have similar compositions in the adjacent rocks implying that reactions can also take place in the absence of contrasted mineral compositions. The continuous change in solid solution composition as well as evidence of transport in both directions indicates diffusion rather than infiltration as the dominant metasomatic mechanism. The small thickness of the margins is also more typical of a diffusion process. Isocon diagrams demonstrate that Al, Ti, and P are perfectly inert components and that no significant mass or volume change occurred during the margin development. Mass balance of this small-scale granulite formation has been estimated with reference to a perfectly inert component (Ti) and assuming that the metabasite bands were compositionally homogeneous. Most of the geochemical variation is mineralogically controlled. Relative to metabasite, Si and Na are increased due to pyroxenes crystallization and to compositional change of plagioclase when it occurs. Potassium decreases because of biotite disappearance. There is no significant variation in U content but Th is slightly decreased. Zirconium and Hf are not affected whereas Nb, Ta and Mn display the largest increase that requires the involvement of a larger volume of metabasite than that observed in the margin. The K/Rb ratio is increased. Fluorine is strongly depleted due to destabilization of amphibole and biotite. The rare-earth element content in margins is either similar to that of the metabasite or intermediate between that of gneiss and metabasite. This last feature is induced by the development of margins at the expense of both adjacent rock types. Saturation surfaces in chemical potential space provide a graphical method for determination of the parameters controlling the diffusion process. In the simplified system CaO-MgO-SiO_2-Al_2O_3-H_2O, these chemical potential diagrams show that evolution along a $(\mu)_{H_2O}$ gradient cannot take into account the three different types of margins. A μ_{H_2O} gradient is thus not prerequisite to the margin development. On the other hand, the succession of zones observed in the different types of margins can be obtained in a μ_{CaO}-μ_{MgO}-μ_{SiO_2} diagram. This suggests that the μ_{SiO_2} gradient existing between the two adjacent rocks controls the margin development in all cases. Moreover, the variable contrast of plagioclase composition between the adjacent rocks is responsible for the presence of one or two pyroxenes in the first zone. The absence of the second clinopyroxene-bearing zone in the third type of margin is likely due to the scarcity of orthopyroxene in the gneiss.

Introduction

Thin centimeter-sized pyroxene-bearing margins occurring at the contact of amphibolites enclosed in acidic rocks have been observed in several granulite terranes. Ramberg (1948) had already reported them from granu-

lites of West Greenland. They have been mentioned by Katz (1969) in granulites of Quebec. Schrijver (1973) described them in the orthopyroxene domain surrounding the Morin anorthosite (Grenville Province) and suggested a bimetasomatic origin. Moreover, Waters (1988), in granulites from Namaqualand (South Africa), considered them as induced by gradients in a_{H_2O} during migmatization and partial melting of adjacent acidic rocks. In Rogaland (Southern Norway), their occurrence has been reported by Tobi et al. (1985) in granulite facies rocks. It thus appears that these margins are frequent in granulite domains and are related to the problem of granulite formation.

Despite their small thickness (5–10 mm), these rocks can be used to make a precise estimate of mass transfer (major and trace elements including rare-earth elements) during the transition of amphibolite into granulite facies. Indeed, since amphibolites can be assumed to have a homogeneous chemistry, the composition of the starting material is known. Moreover, a model will be proposed in order to determine whether an a_{H_2O} gradient is responsible for their formation or if dehydration is simply the result of the reaction.

Regional setting

The Rogaland Province, belonging to the Scandinavian extension of the Grenville Province, is essentially made up of high grade metamorphic rocks, intruded by large anorthositic massifs (Duchesne and Michot 1987; Maijer 1987) (Fig. 1). Three main formations have been recognized in these gneisses (Falkum and Petersen 1980), in order of decreasing age these are: (1) migmatitic banded gneisses; (2) pink granitic gneisses; (3) augen granodioritic gneisses (Bingen 1989; Bingen et al. 1990). An important component of the banded gneisses is formed by layers of mafic rocks (amphibolite, biotite amphibolite, pyroxene amphibolite, hornblende norite) interleaved at decimetric to metric scale with acidic rocks (granitic or charnockitic). The amphibolite horizons are only locally thick enough to be mappable as individual bodies.

The banded gneisses are intensely deformed and have been affected by several episodes of deformation and metamorphism. Hermans et al. (1975) and Jansen et al. (1985) have defined three metamorphic phases: M1, M2, and M3. The M1 stage occurs only as relics and has been dated to 1,200 Ma (Versteeve 1975; Wielens et al. 1980; Priem and Verschure 1982). It corresponds to a regional metamorphism in amphibolite and/or granulite facies conditions ($T = 800\,°C$; $P = 6$–7 kb). The M2 stage is directly linked to the emplacement of the intrusive masses and mainly corresponds to a thermal event ($T = 750$–$900\,°C$) without penetrative deformation except in the vicinity of the main anorthosite intrusions (Egersund-Ogna: Duchesne and Maquil 1987; Ana-Sira: Wilmart and Duchesne 1987) where a synemplacement continuous deformation is observed. It can thus be considered as contact metamorphism in granulite facies conditions. An important temperature gradient is related to the M2 stage and several isograds have been defined with increasing grade towards the intrusions (Hermans et al. 1975): "hypersthene-in" line in leucocratic rocks; "osumilite-in" and "pigeonite-in" isograds (Fig. 1). The "hornblende + quartz-out" isograd is not shown on Fig. 1 and is located between the hypersthene-in and osumilite-in ones. Pressure estimates for M2 stage are still debated: Maijer et al. (1981) and Jansen et al. (1985) consider that this metamorphism is of low pressure (3–4 kbar) on the basis of the osumilite occurrence in the contact aureole of the Bjerkreim-Sokndal lopolith. This interpretation has been questioned by Wilmart and Duchesne (1987) who argued that orthopyroxene-fayalite-quartz assemblages in the upper part of the Bjerkreim-Sokndal lopolith give a pressure of 6–7 kbar with the calibration of Bohlen and Boettcher (1981). There is a fair agreement however between the authors on the conditions of the M3 stage that corresponds to a clockwise retrograde evolution in the P-T plane at about $T = 600\,°C$ and $P = 3$ kbar.

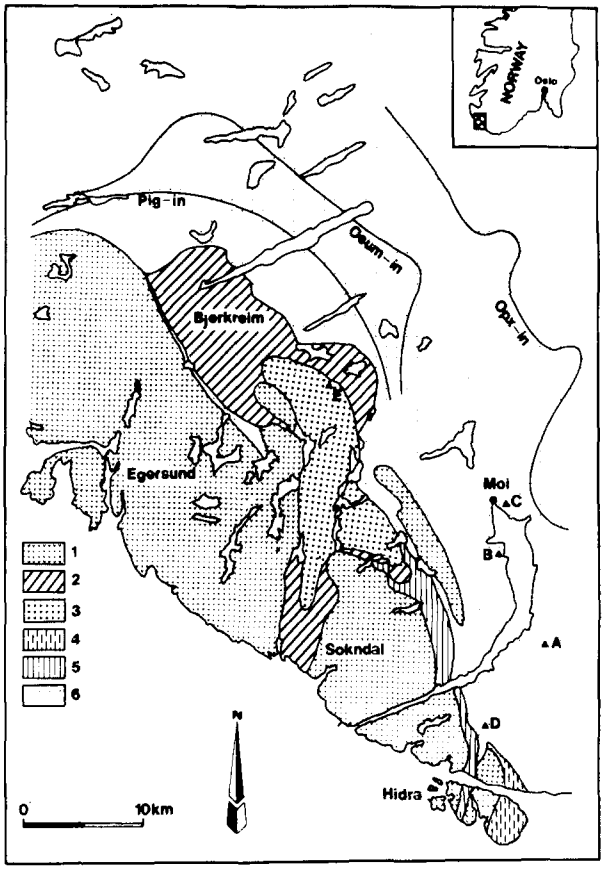

Fig. 1. Schematic geological map of the South Rogaland province (after Hermans et al. 1975). Legend: 1, undifferentiated anorthosite massifs; 2, anorthosite, leuconorite, norite and monzonorite cumulates (lower part of the Bjerkreim-Sokndal lopolith); 3, mangerite and quartz mangerite (upper part of the Bjerkreim-Sokndal lopolith); 4, gneissic charnockitic intrusions; 5, monzonoritic complex (Apophysis); 6, undifferentiated high grade metamorphic rocks. Isograd patterns (*opx*, orthopyroxene; *osum* osumilite; *pig*, pigeonite) after Hermans et al. (1975). Capital letters, *A*–*E*, are for main sites of sampling

Four phases of folding have been distinguished but their correlation with the sequence of metamorphic events has proved difficult (Hermans et al. 1975). According to these authors, the first isoclinal folding is probably coeval with the main phase of migmatization (1,200 Ma). Subsequent folds with axes trending N or NW have been recognized. The granulite facies metamorphism linked to the emplacement of anorthositic intrusive masses appears to post-date the folding.

The pyroxene-bearing margins studied here and occurring at the contacts between basic and acidic rocks have been observed exclusively in the granulite facies domain along the eastern contact of the intrusive masses. According to Tobi et al. (1985), the margins were formed at the expense of the metabasite by a reaction similar to that at the hornblende + quartz-out isograd. In the presence of quartz, amphibole reacts into pyroxenes at a lower temperature than amphibole alone. This explains why quartz-bearing amphibolites are widespread in the amphibolite facies domain outside the orthopyroxene-in isograd and are absent in the granulite domain. Pyroxene-bearing margins have never been observed at the contacts of quartz-

free metabasites and granitic rocks in amphibolite facies rocks. On the other hand, within the hornblende + quartz-out line, these margins occur whenever amphibolites are in contact with acidic rocks, i.e. mainly in banded gneisses but also around basic inclusions in acidic intrusives (quartz mangerite from the upper part of the Bjerkreim-Sokndal lopolith, or from the Apophysis, Breimyrknuten charnockite; Duchesne et al. 1987). The main sites of sampling are displayed on Fig. 1 and described in Table 1.

The occurrence of margins around basic inclusions in the Breimyrknuten charnockite, whose emplacement is clearly post-tectonic (Duchesne et al. 1987) implies that margin development post-dates any deformation. When margins occur in folded metabasites, their thickness remains constant whatever the position in the structure (Fig. 2). This constant thickness also points to a post-tectonic development as gneiss and margin would probably have a similar competence during tectonic processes.

The small thickness (5–10 mm) of the margins is constant from sample to sample. When a metabasic layer is interleaved with acidic rocks, identical margins occur on each side (see Table 1: sample 89-57(1) and 89-57(2) from Flikka). Locally, thin basic horizons have been completely transformed by the reaction and hornblende-bearing metabasites are no longer observable.

Petrography of the margins and related rocks

The margins observed in metamorphic and magmatic rocks are similar. Detailed petrographic study mainly focuses on samples collected in banded gneisses (Fig. 1: A, Flikka; B, Tjellesvik; C, Moi; D, Trolldalen). One occurrence in magmatic rocks (E, Ollestadfjelli in the Bjerkreim-Sokndal lopolith) is also reported.

Metabasites essentially are made up of brown-green hornblende and plagioclase with minor amounts of clinopyroxene, orthopyroxene and biotite. The proportions of these latter three minerals vary from sample to sample (Table 2). Apatite, oxides (ilmenite, magnetite) and zircon occur as accessory phases. K-feldspar is generally absent except in Tjellesvik (point B, Fig. 1) where it forms small xenomorphic crystals around Fe-Ti oxides, plagioclase and biotite, suggesting a secondary origin. Metabasites display a granoblastic texture with foliation defined by hornblende. Thin sections made at different distances from the margin show that they are mineralogically homogeneous.

The sharp contact between metabasite and margin corresponds to the complete disappearance of hornblende and biotite. The margins actually are made up of one or two adjacent zones. Three types of arrangements have been distinguished:-

1. Type 1 : metabastie| plag + opx |plag + cpx|gneiss (Fig. 3)
2. Type 2 : metabasite| plag + opx + cpx |plag + cpx|gneiss
3. Type 3 : metabasite| plag + opx |gneiss

Proportions of pyroxenes (opx, orthopyroxene, cpx, clinopyroxene) and plagioclase (plag) are increased in the first zone (Z1) relative to the original metabasite. Pyroxenes display parallel orientations to the reaction margin suggesting mimetic growth after hornblende (Franssen 1975). A minute amount of biotite is present locally in zone Z1. It occurs as small xenomorphic crystals surrounding the oxides, pointing to a secondary origin related to M3 metamorphic stage (the biotite present in the original metabasite is larger and idiomorphic).

The second zone (Z2), very thin (usual thickness of one mineral grain), is present between the first zone and the acidic gneiss. A peculiar feature of this zone is the cpx grain size which is considerably larger than in Z1 and similar to that of the gneiss (gneiss is not shown on Fig. 3). This evidence, together with the occurrence of quartz inclusions in some large cpx, suggests that an important part of Z2 formed at the expense of the gneiss. Note that these features are observed also in Ollestadfjelli where the basic rock is included in the Bjerkreim-Sokndal quartz

Table 1. Description of the main sites of sampling (capital letters refer to location on Fig. 1)

Locality	Sample no.	Description
A Flikka (LK633708) [a] road E18	89–57(1) 89–57(2)	Banded gneisses: dm-thick layer of metabasite interleaved in charnockitic gneiss, with reaction margins (1) and (2) at each contact of the metabasite with gneiss (first type margin)
	89–58	Identical, only one reaction margin has been sampled (first type margin)
B Tjellesvik (LK583774) road from Moi to Elve	89–75A′	Banded gneisses: reaction margin between a thin basic layer (10 cm) and charnockitic gneiss (second type margin)
C Moi (LK581814) road E18	84–24	Banded gneisses (third type margin)
D Trolldalen (LK575627)	87–7	Banded gneisses at Torsvann
	87–5	Banded gneisses at point 333 m (second type margin)
E Ollestadfjelli (LK446902) (Bjerkreim-Sokndal mas.)	U10	Reaction margin around a basic inclusion in the lopolith quartz mangerite (second type margin)
	U9	Quartz mangerite containing the inclusion

[a] NGU coordinates in zone 32V

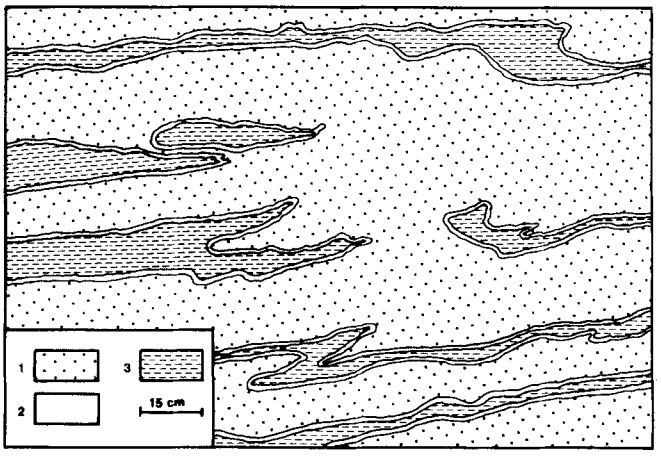

Fig. 2. Reaction margin around folded metabasites in an intensely deformed banded gneiss. Note the constant thickness of the margin whatever the position along the flanks or around the hinges of the folds. 1, gneiss; 2, margin; 3, metabasite

mangerite, thus showing that the enclosing rock was already crystallized when the margins developed. Some large zircons similar to those observed in the acidic rock also are found locally at the limit of the second zone thus confirming the already mentioned process. When thin basic layers have been completely transformed, the margin displays a symmetrical pattern with a central Z1 zone interleaved in two Z2 zones at both contacts with the gneiss.

The margins observed in Moi (Table 2) do not display a second zone with coarse clinopyroxene: they consist only of orthopyroxene and plagioclase with trace amounts of clinopyroxene, locally occurring as a thin film around orthopyroxene.

Some of the samples (Flikka: 89-57, 89-58; Tjellesvik: 89-75A'; Trolldalen: 87-5) have been studied for detailed relationships between the opaque minerals. Magnetite and ilmenite are always present. The proportion of oxides in the zones is similar to that observed in the metabasites, except in Flikka (Fig. 3) where it is somewhat increased. Ilmenite is present either as typical exsolution lamellae in magnetite (sandwich texture) or as individual grains in contact or not with magnetite. In Tjellesvik, hematite exsolutions (lamellae or patches) are abundant in ilmenite (Hematite content close to 20 mol%, following the visual estimation method of Duchesne 1970). Subsolidus reactions (Duchesne 1970) develop a margin of spinelliferous ilmenite and/or a zone in which the hematite exsolution content is decreased at the contact between ilmenite and magnetite grains.

The acidic gneiss is made up of perthitic K-feldspar, antiperthitic plagioclase, quartz, small amounts of pyroxenes (opx and cpx) and oxides (ilmenite and/or magnetite), and apatite and zircon as accessories. K-feldspar has distinctive characters in the different localities. At Flikka, the proportion and size of K-feldspar increased at the direct contact with the reaction border. In contrast, at Tjellesvik and Trolldalen, K-feldspar is less abundant and occurs only as a thin border surrounding quartz grains and sometimes between plagioclase and quartz. This peculiar habit, not observed at Flikka, could have been induced by a very small amount of partial melting during migmatization. Nevertheless, no coarse-grained, unfoliated and discordant patches have been observed in the gneiss adjacent to the margin suggesting that if partial melting occurred it was restricted to grain boundaries. At Moi, K-feldspar is only present as exsolutions in plagioclase and pyroxenes are very scarce. Quartz displays two distinct habits: (1) it most frequently occurs as large ameboid crystals considerably larger than the feldspars or; (2) as scarce small rounded grains included in the feldspars. Unzoned, antiperthitic plagioclase displays lobate contours when in contact with quartz.

Mineral composition

Plagioclase, clinopyroxene and orthopyroxene from six margins as well as amphibole and biotite from metabasites were analyzed by microprobe (Table 3). Figure 4A–D reports the variation of plagioclase and pyroxenes compositions from the metabasite through the gneiss for four samples.

At Flikka (Fig. 4A, B: two margins of the same sample 89-57), the anorthite content of plagioclase is notably different in metabasite (An_{37-40}) compared with adjacent gneiss (An_{24-27}). Plagioclase grains are unzoned. The anorthite content in the margin decreases continuously from the composition observed in the metabasite towards that in the gneiss. Note that in Fig. 4A metabasite plagioclase, measured at 1 cm from the margin has an An_{40} composition whereas in Fig. 4B, at the immediate contact with the margin, it is An_{38}. This slight difference suggests that the compositional evolution of plagioclase occurs on a larger scale than the margin defined on the basis of mineralogical changes.

Similarly, the Fe number of the opx increases progressively from 0.51 in the metabasite towards the value observed in the gneiss (0.58). As cpx occurs only in the second zone of the reaction margin, no continuous composition evolution can be observed for that mineral. Its Fe number is, however, intermediate between the values in metabasite and gneiss. Figure 4B suggests that compositional evolution of cpx is not restricted to the margin.

At Trolldalen (Fig. 4C) and Tjellesvik (Fig. 4D), plagioclase and pyroxene compositions are similar in adjacent gneiss and metabasite and no significant compositional variation is observed in the margins.

These mineral data clearly demonstrate that contrasted mineral compositions in metabasite and gneiss induce a progressive change in the solid solution composition through the margins. It is however worth noting that in half of the samples, pyroxenes and plagioclase have the same composition in metabasite and gneiss implying that a contrasted mineral composition is not prerequisite to the margin development.

In conclusion, any petrogenetic model concerning these zoned reaction margins must account for the following characteristics:-

1. Zone Z1 corresponds to the dehydration of the metabasite (hornblende and biotite react into pyroxenes); these

Table 2. Petrographical composition of metabasites, margins, and adjacent acidic gneisses (≈ symbol means scarce mineral)

Locality	Metabasite (Z0)	Z1	Z2	Gneiss adjacent Z2	Gneiss
Flikka	Hornblende			K-feldspar rich	K-feldspar
	Opx	Opx		Opx	Opx
	Cpx		Cpx	Cpx	Cpx
	Plag (An_{40})	Plag	Plag	Plag	Plag (An_{26})
	Biotite	≈Biotite		Quartz	Quartz
	Apatite	Apatite	Apatite	Apatite	Apatite
	≈Magnetite	Magnetite	Magnetite	≈Magnetite	≈Magnetite
	Ilmenite	Ilmenite	Ilmenite	Ilmenite	Ilmenite
	Zircon	Zircon	Zircon	Zircon	Zircon
Tjellesvik	Hornblende				
	Plag (An_{31})	Plag	Plag		Plag (An_{31})
	Opx	Opx			Opx
	Cpx	Cpx	Cpx		Cpx
	Hemoilmenite	Hemoilmenite	Hemoilmenite		Hemoilmenite
	Magnetite	Magnetite	Magnetite		Magnetite
	≈Biotite	≈Biotite			Quartz
	≈K-feldspar	≈K-feldspar	≈K-feldspar		K-feldspar
	Zircon	Zircon	Zircon		Zircon
	Apatite	Apatite	Apatite		Apatite
Moi	Hornblende				Quartz
	Biotite	≈Biotite			K-feldspar (antipecthite)
	Plag (An_{45})	Plag			Plag (An_{20})
	Oxide	Oxide			Oxide
	Opx	Opx			≈Opx
	Cpx	≈Cpx			≈Cpx
	Apatite	Apatite			Apatite
	Zircon	Zircon			Zircon
Trolldalen	Hornblende				K-spar
	Plag (An_{30})	Plag	Plag		Plag (An_{30})
	Cpx	Cpx	Cpx		Cpx
	Opx	Opx			Opx
	Apatite	Apatite	Apatite		Apatite
	Zircon	Zircon	Zircon		Zircon
	Magnetite	Magnetite	Magnetite		Magnetite
	Ilmenite	Ilmenite	Ilmenite		Ilmenite
	≈Biotite	≈Biotite			Quartz
Ollestadfjelli	Hornblende				
	Plag	Plag	Plag		Plag
	Cpx	Cpx	Cpx		Cpx
	Opx	Opx			Opx
	≈Biotite	≈Biotite			K-feldspar
	Apatite	Apatite	Apatite		Apatite
	Zircon	Zircon	Zircon		Zircon
	Oxide	Oxide	Oxide		Magnetite
					Ilmenite
					Quartz

margins therefore correspond to a small-scale granulite formation;

2. The margins are most frequently composed of two zones, the first one (Z1) containing either orthopyroxene only or both pyroxenes, and the second one (Z2), clinopyroxene. When only one zone occurs, it consists of opx. Plagioclase is always present;

3. Zone Z1 develops at the expense of the metabasite whereas zone Z2 is formed at the expense of both Z1 and gneiss, which implies that growth of the margins occurs in both directions;

4. The different zones are separated by sharp fronts and the number of phases is reduced compared to metabasite and gneiss;

5. They show a small and constant thickness;

6. When adjacent rocks show contrasting mineral compositions, the compositions of the solid solutions evolve continuously from the value in the metabasite to that in the gneiss, with no abrupt change across Z1-Z2 front.

Features 2 to 6 are typical of metasomatic rocks (Korzhinskii 1970; Joesten 1977; Fonteilles 1978) and feature 3, as well as the lack of abrupt change in solid solutions across Z1-Z2 front, is typical of diffusion metasomatic rocks (Hofmann 1972).

Mass transfer evaluation

Introduction

In early geochemical studies, it was deduced from direct comparison of granulites and their supposed amphibolite equivalents that granu-

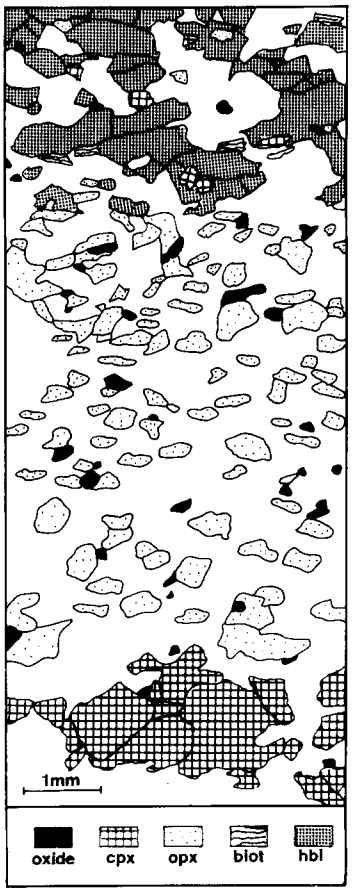

Fig. 3. Reaction margin at the contact between metabasite and gneiss (not shown on the figure). The amphibolite (*upper* part of the sketch) is in sharp contact with zone Z1 made up of plagioclase, opx and opaques. Note zone Z2 (*lower* part of the sketch) is characterized by coarse-grained cpx as the only pyroxene. Note the grossly parallel orientation of opx with the contact between zones. Plagioclase is in *white*. (sample 89-57(1), Flikka)

lite terranes are depleted in some large-ion-lithophile elements (LILE), more precisely in K, Rb, U and Th with concomitant increase of the K/Rb and Th/U ratios (Lambert and Heier 1967; Heier and Thorensen 1971; Weaver and Tarney 1983). More recent papers have shown that this depletion is not systematic (Sighinolfi et al. 1981; Iyer et al. 1984; Barbey and Cuney 1982). A large data base has been used by Rudnick et al. (1985) to test the behavior of Rb, K, Th and U in granulites. According to these authors, U seems to decrease whereas Th could be constant. Moreover, the K/Rb ratio increases in the low K granulites but remains unchanged in the high K granulites. Following these authors, this variable behavior is induced by the relative stability of biotite and K-feldspar: in high K granulites, K-feldspar is the potassic phase and is stable in granulite facies conditions. In low K rocks, biotite is present and will react into K-feldspar in granulite conditions with a change in the K/Rb ratio. Most frequently, element mobilities have been estimated by simple comparison of the element content in granulite and amphibolite terranes with, in most cases, no reference to a fixed component. Moreover, estimates made on regional scale cannot account for heterogeneity in the protolith composition nor for volume variation (if any) during transformation and deformation. The zoned reaction margins studied in this paper are not representative of regional granulite facies but the protolith of each margin is known and is of constant composition : metabasites as well as their equivalent in the amphibolite facies domain (located more eastwards) are mineralogically very homogeneous. Moreover, in the amphibolite facies no reaction or distinctive layer can be observed at the contact with the gneiss (hornblende is stable in the presence of quartz in the amphibolite facies conditions).

Petrographic data have shown that part of zone Z2 was formed at the expense of the gneiss (see above): a mass transfer evaluation made with these margins thus strictly is not representative of granulite formation. This is especially true for some trace elements as scarce zircon in the gneiss has been observed in zone Z2. These

Table 3. Selected electron-probe analyses of plagioclase, orthopyroxene, clinopyroxene [sample 89-57(2)]

	Plagioclases		
	1	2	3
SiO_2	56.32	59.84	61.26
Al_2O_3	27.12	25.01	23.73
FeO	0.19	0.24	0.11
CaO	8.64	6.64	4.73
Na_2O	6.61	7.63	8.52
K_2O	0.33	0.64	0.51
Total	99.21	100.00	98.86
		8 Oxygens	
Si	2.551	2.674	2.749
Al	1.448	1.317	1.255
Fe	0.007	0.009	0.004
Ca	0.419	0.318	0.228
Na	0.580	0.662	0.741
K	0.019	0.037	0.029
Ab	57.0	65.1	74.3
Or	1.9	3.6	2.9
An	41.2	31.3	22.8

	Orthopyroxenes			Clinopyroxenes	
	4	5	6	7	8
SiO_2	50.62	49.84	49.11	50.40	50.50
TiO_2	0.10	0.18	0.19	0.23	0.17
Al_2O_3	0.91	1.05	0.70	1.92	1.48
FeO	30.60	31.36	34.58	13.67	14.52
MnO	0.95	0.78	0.97	0.44	0.40
MgO	16.43	16.23	13.49	12.05	10.73
CaO	0.66	0.81	1.02	20.32	20.97
Na_2O	0.04	0.00	0.00	0.41	0.50
Total	100.31	100.25	100.06	99.44	99.27
			6 Oxygens		
Si	1.964	1.945	1.955	1.932	1.950
Al IV	0.036	0.048	0.033	0.068	0.050
Al VI	0.006	–	–	0.019	0.017
Ti	0.003	0.005	0.006	0.007	0.005
Fe	0.993	1.023	1.151	0.438	0.469
Mg	0.950	0.944	0.800	0.688	0.617
Mn	0.031	0.026	0.033	0.014	0.013
Ca	0.028	0.034	0.043	0.834	0.867
Na	0.003	0.000	0.000	0.030	0.037
Fm	0.519	0.526	0.597	0.397	0.438
Wo	1.4	1.7	2.1	42.2	44.1
En	47.5	46.6	39.5	34.9	31.4
Fs	51.2	51.8	58.4	22.9	25.4

The number of the analysis refers to Fig. 4; analyses made at the CAMST (University of Louvain – J. Wautier, analyst) with a Camebax microprobe (wavelength dispersive spectrometer) 15 kV, 20 nA, data reduced using a ZAF correction program from CAMECA

Table 3. (continued) Selected electron-probe analyses of biotite, and amphibole [sample 89-57(2)]

	Amphiboles		Biotites	
	9	10	11	12
SiO_2	41.21	40.98	36.55	36.98
TiO_2	2.45	1.74	4.85	4.60
Al_2O_3	10.83	10.95	12.99	13.21
FeO	16.01	16.56	16.09	16.28
MnO	0.27	0.30	0.00	0.17
MgO	10.63	10.75	13.66	13.55
CaO	11.05	11.16	0.00	0.00
Na_2O	2.28	2.34	0.01	0.08
K_2O	1.74	1.74	9.93	9.44
F	0.85	1.73	1.77	1.33
Cl	0.04	0.06	0.06	0.05
H_2O	1.54	1.13	3.06	3.29
F = O	− 0.36	− 0.73	− 0.75	− 0.56
Cl = O	− 0.01	− 0.01	− 0.01	− 0.01
Total	98.53	98.70	98.21	98.40
		[a]	22 Oxygens	
Si	6.280	6.244	5.602	5.639
Al IV	1.720	1.756	2.347	2.361
Al VI	0.221	0.212	–	0.013
Ti	0.284	0.201	0.559	0.527
Fe^{3+}	0.308	0.463	–	–
Fe^{2+}	1.734	1.643	2.063	2.076
Mn	0.036	0.037	0.000	0.022
Mg	2.417	2.444	3.121	3.080
Ca	1.804	1.822	0.000	0.001
Na	0.677	0.696	0.003	0.023
K	0.339	0.339	1.942	1.837
OH	1.579	1.151	3.126	3.346
F	0.412	0.834	0.858	0.640
Cl	0.009	0.015	0.016	0.014

[a] Number of oxygens on the basis of 13 cations except Ca, Na, K

limitations will be considered before making any general conclusion on mass transfer.

Sample preparation

Seven samples from the various localities have been selected for whole rock analysis (major and trace elements). In each case the metabasite and the reaction margin have been considered as well as the adjacent acidic gneiss. In rock 89-57 two margins [89-57(1) and 89-57(2)], on each side of a metabasite layer, have been sampled together with their respective adjacent gneisses. It must be pointed out that these latter have variable compositions and may show local heterogeneities which have justified the sampling of a K-feldspar-rich layer adjacent to margin 89-57(1).

Each sample (usually of 1 dm^3 size) has been cut at right angles to the margin orientation in 1 cm thick slices. The sharp contrast in mineral compositions between the various rocks (metabasite, margin and gneiss) has made it possible to cut homogeneous and representative samples (15–30 gm) of each rock type. A distinction within each margin between zones Z1 and Z2 has, however, not been possible. The analyses are reported in Table 4. The interpretation of the compositions in terms of provenance of the material or influence of migmatitic processes has been discussed by Wilmart et al. (1987) for similar metabasites and acidic gneisses. The present paper will focus on the chemical changes due to the granulite formation.

Methods of evaluation

In most geochemical studies of granulite terranes, an element is considered mobile when its content decreases or increases in granulites compared to its content in its supposed amphibolite protolith. This mobility concept is distinct from that proposed by Korzhinskii (1959) and Thompson (1970) in which an element is perfectly mobile when its chemical potential (μ) is controlled by conditions external to the system and has thus the same status as P and T in determining the equilibrium paragenesis. The perfectly mobile components are opposed to the inert ones whose μ are controlled at constant P and T by the paragenesis and the μ of the perfectly mobile components. To fill the gap between these geochemical and thermodynamic concepts, Fonteilles (1978) has defined perfectly inert components as inert components whose contents, or better, ratios of contents have not been modified during transformation. Perfectly inert components are convenient for mass transfer evaluation because they provide a fixed reference to which the behavior of other elements can be compared.

Gresens (1967) proposed a basic formula for analyzing changes in concentration and volume during metasomatic reactions:

$$X_n = [f_v(\rho^b/\rho^a)\ C_n^b - C_n^a]100$$

in which a and b refer to the rock before and after transformation; f_v, to the volume ratio V^b/V^a and ρ is for the specific gravity. With this equation, composition-volume diagrams (X_n versus arbitrary values of f_v) can be obtained for the different components and the perfectly inert ones are those which intersect at a common value of f_v for $X_n = 0$.

Grant (1986) rearranged Gresens' equation into a linear relationship between the concentration of one component before and after alteration:

$$C_i^b = \frac{M^a}{M^b}(C_i^a + \Delta C_i)$$

where a and b refer to the rock before and after transformation, M^a/M^b is the ratio of equivalent masses and C_i is for the concentration of component i. Components showing no relative gain or loss define an "isocon" ($C_i^b = (M^a/M^b)\ C_i^a$) whose slope gives the mass change (M^a/M^b) during transformation. This method provides an objective way of determining perfectly inert components.

Isocon diagrams (Fig. 5) show that in all samples, the best-fit isocon is obtained with Ti, Al and P. This means that either these elements are perfectly inert or that they have been changed in the same way (i.e, they are geochemically coupled). As these elements are included in different minerals (Ti is in biotite, amphibole and oxides; Al is mainly in feldspar; P in apatite), the second hypothesis is very unlikely and we will consider them as perfectly inert. It is also worth noting that Fe and Mg are usually on the best-fit isocon or close to it. Isocon slopes range from 0.95 to 1.05 (except for sample U10 where it is 0.80), suggesting that no significant mass change occurred during the reactions.

Volume changes can be assessed using best-fit and constant-volume isocons ($C_i^b = \rho^a/\rho^b \cdot C_i^a$; Grant 1986) if specific gravities are known. Constant volume is shown when both isocons have the same slope. Specific gravities of four samples have been measured using a Berman balance (89-58; 89-57(1); 89-57(2); 89-75A') (Table 5). Constant volume isocons are identical to best-fit isocons for samples 89-75A' and 89-57(2) and close to it for the two other samples (Fig. 5; Table 5) demonstrating that margin development occurred with no significant volume change.

In Fig. 5, relative gains and losses of major elements are given by their displacement from the isocon. Nevertheless, gains and losses are best measured by comparing the concentration change of one component to its initial concentration ($\Delta C_i/C_i^a$). This can be done by assuming constant mass, constant volume or referring to one perfectly inert component. The last method has been chosen because time-consuming measures of specific gravities are avoided and it takes into account variations due to concentration and dilution effects (this is not the case for the mass constant method). The component TiO_2 has been selected from among the perfectly inert

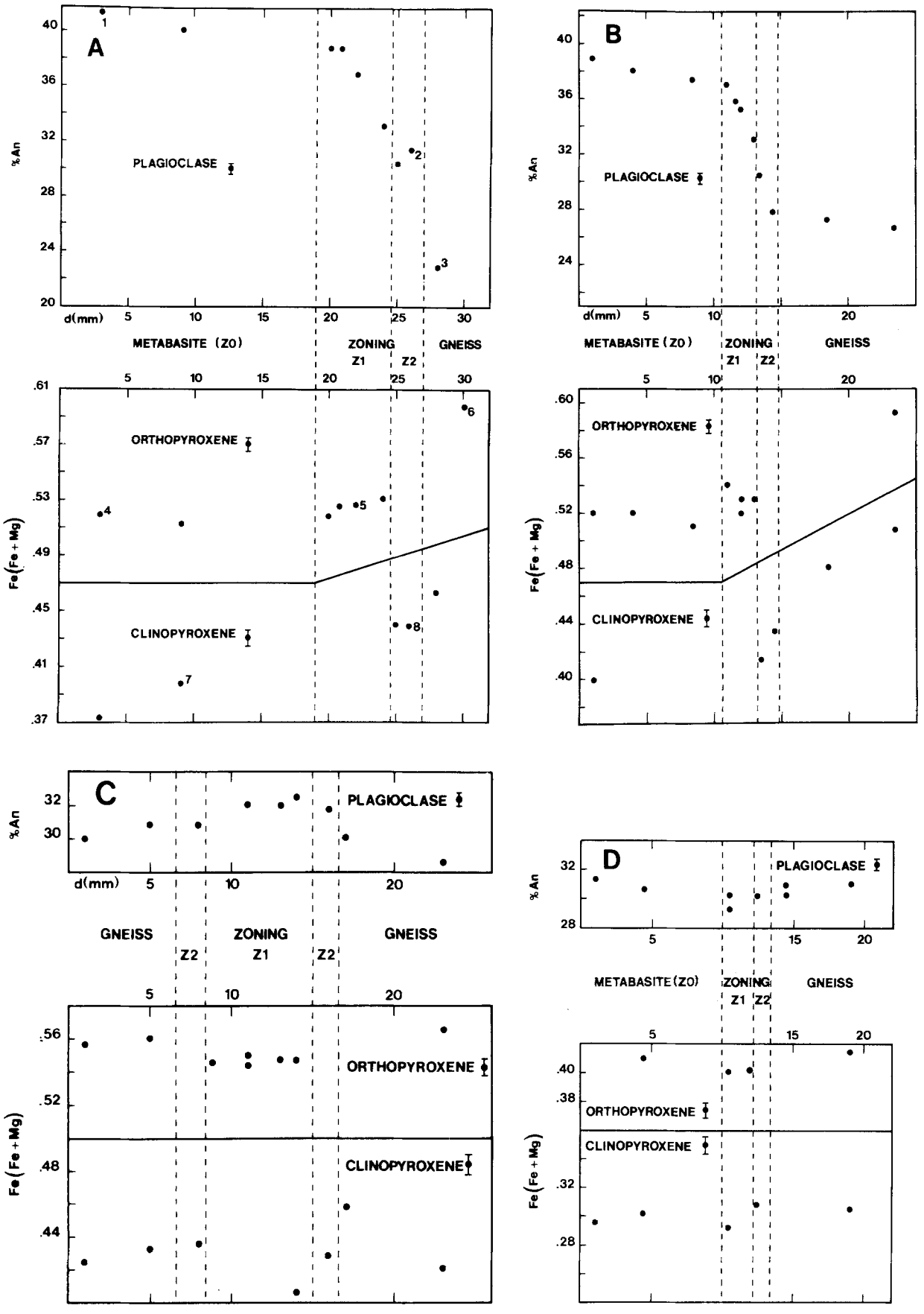

Fig. 4A–D. Mineral composition (anorthite content for plagioclase and Fe/(Fe + Mg) – Fe number – for pyroxenes) across the reaction margin (distance in mm). Error bars (1σ) are for analytical precision: **A** sample 89-57(2) (Flikka) – type 1; analysis numbers refer to Table 3; **B** sample 89-57(1) (Flikka) – type 1; **C** sample 87-5 (Trolldalen) – type 2; **D** sample 89-75A′ (Tjellesvik) – type 2

because its analytical precision is excellent. Errors on mass transfer calculations have been estimated following the principle of error propagation (Topping 1966).

Major and trace elements

Results are displayed in Table 6 and on Fig. 6 (major elements) and Fig. 7 (trace elements). The propagated errors are variable from element to element. They are relatively low for the major elements except Na which is not precisely analyzed by XRF. Values for U, Nb and Ta display important errors due to their very low content in samples. Errors being considered, the following features can be pointed out:-

1. Silica usually increases in the range of + 10% to + 22% with one value reaching + 40%. There is only one exception in sample 89-75A' where this element remains constant;
2. Sodium is significantly enriched in all samples except 89-75A';
3. Manganese is strongly increased in all samples with gains from + 15% to + 73% and, interestingly, its content is higher in margins than in both metabasite and gneiss;

Table 4. Major (%) and trace (ppm) element composition of margin and corresponding gneiss and metabasites [for sample 89-57, the two margins (1) and (2) as well as the K-feldspar(KF)-rich gneiss adjacent to margin (1) are also presented]. Sample numbers refer to Table 1

	89-57 Metabasite	89-57(1) Margin	89-57(1) KF-rich gneiss	89-57(1) Gneiss	89-57(2) Margin	89-57(2) Gneiss	89-58 Metabasite	89-58 Margin	89-58 Gneiss
SiO_2	48.27	53.70	73.32	70.18	54.17	63.90	49.58	55.28	68.33
TiO_2	1.22	1.13	0.45	0.70	1.12	1.00	1.18	1.13	0.75
Al_2O_3	15.65	14.99	13.29	13.33	14.92	15.57	15.30	14.84	13.47
Fe_2O_3t	12.89	12.87	2.71	5.93	13.11	7.14	12.61	11.99	6.82
MnO	0.19	0.30	0.05	0.08	0.31	0.10	0.20	0.27	0.10
MgO	7.57	5.25	0.66	0.85	5.08	1.06	7.35	4.90	1.00
CaO	9.99	7.50	2.56	2.83	7.17	3.65	9.68	7.76	3.26
Na_2O	2.70	4.23	2.00	2.98	4.23	3.82	2.48	3.55	3.11
K_2O	1.36	0.49	5.55	3.49	0.50	4.07	1.39	0.63	3.46
P_2O_5	0.21	0.21	0.14	0.24	0.22	0.28	0.21	0.24	0.25
Total	100.05	100.67	100.73	100.60	100.82	100.59	99.96	100.59	100.54
U	0.23	< 0.14	0.25	0.46	0.18	0.60	0.40	0.33	0.35
Th	0.82	0.38	0.48	0.43	0.51	1.04	0.80	0.56	0.48
Th/U	3.6		1.9	0.9	2.8	1.7	2.0	1.7	1.4
Zr	96	187	254	377	215	514	100	211	401
Hf	2.7	5.0	8.5	11.9	6.2	15.4	2.7	6.7	12.4
Zr/Hf	36	37	30	32	35	33	37	31	32
Nb	< 6	12	< 6	< 6	15	17	< 6	11	9
Ta	0.26	0.74	0.34	0.27	1.05	1.16	0.36	0.81	0.37
Nb/Ta		16			14	15		14	24
Rb	55	14	137	90	12	98	67	20	87
K/Rb	205	291	336	322	346	345	172	262	330
Sr	228	186	211	185	188	213	222	184	176
Ba	153	116	1,192	796	116	906	198	143	714
K/Ba	74	35	39	36	36	37	58	37	40
V	244	165	< 25	< 25	152	38	232	162	< 25
Cr	113	70	4[a]	5[a]	75	6[a]	124	85	11[a]
Ni	100	51	< 25	< 25	56	30	92	53	< 25
Zn	102	134	< 25	62	141	63	101	111	80
Sc	34.7	25.4	4.7	6.5	31.0	11.4	33.3	30.7	14.5
La	13.6	17.7	15.4	25.9	23.2	38.9	13.7	25.1	31.5
Ce	34.9	35.0	27.8	50.4	47.7	81.0	35.2	58.6	68.7
Nd	20.2	19.4	13.6	24.5	26.0	41.0	19.4	35.0	36.1
Sm	5.03	4.74	3.16	5.00	6.48	8.67	4.89	8.50	7.97
Eu	1.52	1.61	2.01	2.01	1.67	2.50	1.53	1.94	2.27
Tb	0.94	0.79	0.39	0.59	1.16	1.29	0.89	1.44	1.29
Yb	3.38	3.10	1.27	1.65	4.80	4.10	3.30	5.10	3.89
Lu	0.52	0.46	0.18	0.23	0.72	0.57	0.52	0.75	0.58
Y	33	39	7	16	48	41	31	53	40
(La/Yb)N	1.8	0.8	20	10	0.5	5	1.8	0.6	4
Eu/Eu*	0.88	1.01	2.02	1.29	0.76	0.88	0.91	0.68	0.86
∑REE	80	83	64	110	112	178	79	136	152

Major elements and Zr, Rb, Sr, Ba, V, Cr, Ni, Zn, Nb and Y analysed by XRF (G. Bologne, ULG); U, Th, Hf, Ta, Sc and REE by NAA [J. Hertogen, KUL, for samples 89-57(1) and (2), 89-58, 89-75A', 87-7, 87-5; J.L. Joron and E. Wilmart, CEA, Saclay, for samples U10, U9, and 84-24] as well as elements marked[a]. F was determined by PIGE (I. Roelandts, ULG) (Roelandts et al. 1987)

Table 4 (continued)

	89-75A' Metabasite	89-75A' Margin	89-75A' Gneiss	87-7 Metabasite	87-7 Margin	87-7 Gneiss	87-5 Metabasite	87-5 Margin	87-5 Gneiss
SiO_2	47.79	50.81	69.43	44.91	49.83	75.55	49.69	53.12	75.18
TiO_2	2.25	2.38	0.38	2.55	2.48	0.30	1.74	1.57	0.51
Al_2O_3	14.14	14.65	15.75	15.02	15.68	12.62	13.28	13.43	11.22
Fe_2O_3t	14.46	14.87	3.16	17.28	16.46	2.50	14.92	14.48	4.64
MnO	0.22	0.30	0.05	0.27	0.34	0.02	0.26	0.27	0.04
MgO	6.73	5.83	1.13	7.60	6.26	0.19	6.86	5.57	0.43
CaO	9.47	5.69	4.10	9.81	5.26	1.53	10.41	7.75	1.15
Na_2O	2.99	3.60	3.65	1.83	3.84	2.80	3.44	4.58	2.28
K_2O	1.09	0.81	1.53	1.79	0.21	4.69	0.69	0.47	4.84
P_2O_5	0.39	0.39	0.17	0.33	0.36	0.04	0.23	0.18	0.16
Total	99.53	99.32	99.53	100.11	99.36	100.19	100.37	100.28	100.24
U	0.27	0.43	< 0.15	< 0.15	0.20	0.41	0.75	0.49	1.60
Th	0.62	0.42	0.11	0.48	0.32	0.38	1.19	0.65	18.40
Th/U	2.3	1.0			1.6	0.9	1.6	1.3	11.5
Zr	155	166	89	162	140	250	88	68	455
Hf	4.5	4.7	2.8	4.0	4.0	8.1	2.9	2.3	15.7
Zr/Hf	34	35	32	41	35	31	30	30	29
Nb	6	7	< 6	3	12	2	4	25	2
Ta	0.39	1.05	0.06	0.24	0.54	0.07	0.40	1.90	0.23
Nb/Ta	15	7		13	22	29	10	13	9
Rb	15	17	22	104	23	130	17	8	166
K/Rb	603	396	577	143	76	300	337	488	242
Sr	363	529	700	179	165	123	141	212	176
Ba	234	294	624	165	161	976	95	178	1244
K/Ba	39	23	20	90	11	40	60	22	32
V	315	310	28	393	379	< 25	389	286	< 25
Cr	133	132	< 10[a]	111	128	39	178	161	< 25
Ni	52	39	< 25	85	38	< 25	68	47	< 25
Zn	113	140	33	150	159	33	124	173	42
Sc	38.9	27.1	4.0	38.6	28.7	3.4	50.8	44.7	68.3
La	18.4	15.4	12.1	9.9	15.9	13.8	12.3	12.6	68.3
Ce	51.8	34.0	20.9	27.6	29.9	17.7	35.7	33.3	124.0
Nd	35.1	18.8	8.3	21.3	15.9	6.8	24.1	25.8	46.2
Sm	8.3	4.1	1.5	6.1	3.4	1.4	6.5	8.3	6.7
Eu	2.43	1.33	1.14	2.19	1.90	1.57	1.84	1.42	0.94
Tb	1.34	0.55	0.14	1.17	0.51	0.14	1.27	1.89	0.48
Yb	4.00	1.61	0.27	3.97	2.30	0.50	5.00	8.00	1.18
Lu	0.61	0.25	0.05	0.56	0.38	0.08	0.75	1.21	0.20
Y	47	19	< 6	37	21	4	58	89	4
(La/Yb)N	3	6	30	2	5	18	2	1	70
Eu/Eu*	0.60	0.74	2.26	0.64	0.97	2.62	0.46	0.24	0.41
∑REE	122	76	44	73	70	42	87	93	248
F				4,276	679	< 25	3758	428	184

4. Aluminium and Fe are almost constant; small but significant gains of Fe are observed in samples U10 and 89-57(2);
5. A small decrease in Mg occurs for several samples and Ca is decreased in all samples, except in U10 where it is increased;
6. Potassium is depleted from − 25% down to − 89%, except in U10 where it is slightly increased, this feature probably being due to incorporation in zone Z2 of this sample of K-feldspar from the gneiss (see the petrographic section);
7. The behavior of P is variable from sample to sample : it is slightly increased or decreased.

The behavior of trace elements is not as consistent as that of major elements (Fig. 7) :-

1. Uranium displays no significant variation whereas Th is significantly decreased in a few samples but increased up to + 35% in U10;
2. Tantalum displays a strong increase in all samples and so does Nb in most samples: maximum values can attain 4 to 6 times the value in the metabasite (sample 87-5), as for Mn both elements are strongly enriched in margins relative to metabasite and gneiss;
3. Zirconium and Hf have a parallel behavior (nearly constant Zr/Hf ratios – Table 4) and display a significant increase in only three cases. This increase is, however, correlated with a high Zr content in the adjacent gneiss and is likely due to the incorporation of zircon from the gneiss (part of zone Z2 developed at the expense of the gneiss: see petrographic section).
4. Rubidium is unaffected in some samples but, more frequently, strongly decreased from − 48% down to

Table 4 (continued)

	U10 Metabasite	U10 Margin	U9 Gneiss	84-24 Metabas	84-24 Margin
SiO_2	46.53	52.81	62.51	45.52	48.90
TiO_2	2.94	2.38	0.82	2.66	2.59
Al_2O_3	12.43	11.76	14.98	15.06	15.76
Fe_2O_3t	18.18	17.04	9.22	16.33	15.48
MnO	0.25	0.34	0.15	0.20	0.25
MgO	5.74	4.33	0.94	7.12	6.66
CaO	10.32	9.29	3.78	9.32	5.82
Na_2O	2.78	3.95	3.35	2.46	3.90
K_2O	0.71	0.64	3.78	1.64	0.70
P_2O_5	0.73	0.63	0.26	0.64	0.61
Total	99.00	101.68	99.79	100.95	99.62
U	0.79	0.86	0.36	0.85	1.28
Th	2.01	2.20	0.83	1.64	1.72
Th/U	2.54	2.56	2.31	1.93	1.34
Zr	306	268	424[a]	192	208
Hf	7.7	6.9	10.0	4.8	5.8
Zr/Hf	40	39	42	40	36
Nb	17	37	11	7	11
Ta	0.88	2.18	0.62	0.44	0.90
Nb/Ta	19	17	18	16	12
Rb	11	10	62[a]	117	17
K/Rb	536	531	505	116	342
Sr	228	246	230[a]	279	279
Ba	204[a]	392[a]	1517[a]	403	291
K/Ba	29	14	21	34	20
V	–	–	–	273	344
Cr	158[a]	132[a]	29[a]	44	52
Ni	31[a]	15[a]	2[a]	78[a]	73[a]
Zn	339[a]	405[a]	246[a]	168	219
Sc	48.7	45.4	22.2	35.3	35.0
La	32.60	41.40	35.20	21.50	24.00
Ce	74.20	94.90	81.40	52.40	53.00
Nd					
Sm	11.90	16.60	11.70	8.10	7.90
Eu	3.34	3.18	6.10	2.90	2.07
Tb	2.04	2.76	1.74	1.36	1.19
Yb	8.48	9.76	5.39	5.00	3.63
Lu					
Y	90	117	58	65	58
∑REE	133	169	142	91	92
(La/Yb)					
Eu/Eu*	0.83	0.57	1.60	1.06	0.80
F	4501	792		6798	1824

– 85%. Both Rb and K have similar behavior but Rb is generally more depleted than K, which induces an increase of K/Rb (Table 4);
5. Both Sr and Ba display the highest increase in the same three samples but their behaviors are not necessarily parallel with that of Ca inasmuch as the strong gain of Ba and Sr in sample 87-5 is associated with a depletion in Ca;
6. Contents of V, Cr and Sc are not very much affected by the margin development: they mostly show slight losses;
7. Nickel significantly decreases in most cases down to about 50%, whereas Zn is increased up to about 50%;
8. Fluorine is always strongly depleted.

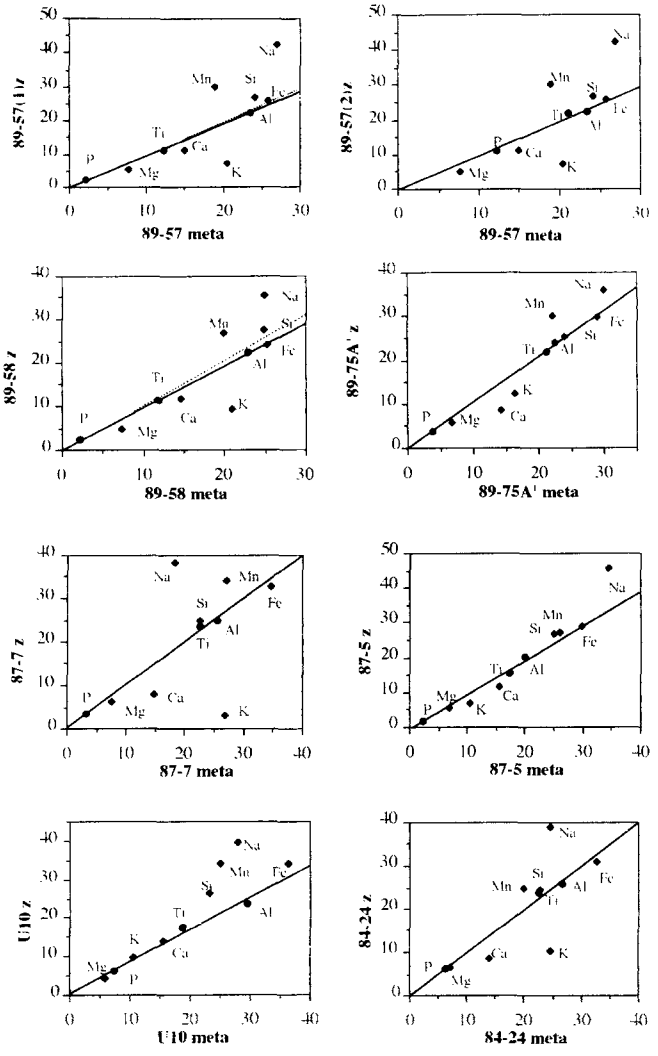

Fig. 5. Isocon diagrams (Grant 1986: see text for explanation) for all metabasites (*x*-coordinate) and corresponding margins (*y*-coordinate). Data are plotted as weight percent of the oxides: component concentrations have been scaled in order to be shown in the range 0 to 40 wt% (0.5 SiO_2, 10 TiO_2, 1.5 Al_2O_3, 2Fe_2O_3, 100 MnO, 1 MgO, 1.5 CaO, 10 Na_2O, 15 K_2O, 10 P_2O_5). This avoids neglecting variations in components with low concentrations (Grant 1986). *Solid lines* are best-fit isocons and *dotted lines*, constant-volume isocons

Table 5. Values of specific gravities (g) measured for 4 samples of metabasites and corresponding margins. The volume ratio, V_z/V_{meta} (z, margin; meta, metabasite) deduced from best-fit isocons (Grant 1986) is also given

Sample no.	89-57(1)	89-57(2)	89-58	89-75A'
g Margin[a]	3.10	3.10	3.04	2.82
g Metabasite	3.10	3.10	3.10	2.86
V_z/V_{meta}	1.05	1.00	1.06	0.96

[a] Average of 3 measures on a Berman balance

Selected REE patterns of metabasites, margins and gneisses are reported in Table 4 and Fig. 8. Note the peculiar REE distribution with a strong positive anomaly in some gneisses, a feature not uncommon in migmatitic

Table 6. Mass transfer estimates using TiO_2 as a fixed reference (see text). Gains and losses are expressed as percentages of the metabasite composition. The last column gives the average absolute error (1σ)

	89-57(1)	89-57(2)	89-58	89-75A'	84-24	87-7	U10	87-5	Error
SiO_2/TiO_2	20	22	16	1	10	14	40	19	1.4
Al_2O_3/TiO_2	3	4	1	− 2	7	7	17	12	2.1
Fe_2O_3t/TiO_2	8	11	1	− 3	− 3	− 2	16	7	1.2
MnO/TiO_2	66	73	41	26	25	27	56	15	2.1
MgO/TiO_2	− 25	− 11	− 30	− 18	− 4	− 15	− 7	− 10	3.5
CaO/TiO_2	− 19	− 22	− 16	− 43	− 36	− 45	11	− 17	0.9
Na_2O/TiO_2	69	71	50	14	64	115	75	47	8.6
K_2O/TiO_2	− 61	− 60	− 53	− 29	− 57	− 89	13	− 25	2.9
P_2O_5/TiO_2	9	16	18	− 4	0	15	4	− 15	3.2
U/TiO_2	> − 35	− 15	− 14	50	53	33	34	− 27	80
Th/TiO_2	− 50	− 32	− 27	− 37	6	− 32	35	− 39	15
Zr/TiO_2	110	144	120	1	11	1	8	− 14	8
Hf/TiO_2	103	154	158	− 1	24	3	10	− 12	13
Nb/TiO_2	> 116	> 172	> 92	10	61	264	169	575	89
Ta/TiO_2	212	346	131	160	106	144	207	426	58
Ba/TiO_2	− 18	− 17	− 25	19	− 26	0	137	108	10
Rb/TiO_2	− 73	− 76	− 69	7	− 85	− 77	12	− 48	5
Sr/TiO_2	− 12	− 10	− 13	38	3	− 5	33	67	4
V/TiO_2	− 27	− 32	− 27	− 7	29	− 1		− 19	4
Cr/TiO_2	− 33	− 28	− 28	− 6	21	19	3	0	14
Ni/TiO_2	− 45	− 39	− 40	− 29	− 3	− 54	− 39	− 23	12
Zn/TiO_2	42	51	15	− 5	34	9		55	9
Sc/TiO_2	− 21	− 3	− 4	− 34	2	− 24	15	− 3	2
$\Sigma REE/TiO_2$	3	52	79	− 41	3	− 1	57	17	4
Eu/TiO_2	14	19	32	− 48	− 27	− 11	17	15	4
F/TiO_2					− 72	− 84	− 78	− 87	3

Caculation of the propagated error was done by considering the following values of the standard deviation for each element (in percent for major elements and ppm for traces). Elements measured by XRF (G. Bologne, personal communication): SiO_2, 0.26; TiO_2, 0.01; Al_2O_3, 0.16; Fe_2O_3, 0.04; MnO, 0.002; MgO, 0.16; CaO, 0.04; Na_2O, 0.11; K_2O, 0.03; P_2O_5, 0.006; Ba, 10; Co, 4; Cr, 10; Nb, 1.4; Ni, 6; Rb, 3.5; Sr, 5.5; V, 7; Y, 4; Zn, 6.5; Zr, 6.2. Elements measured by NAA (J. Hertogen, personal communication): Hf, 0.22; Ta, 0.06; U, 0.16; Th, 0.10; Sc, 0.58; ΣREE, 2.2; Eu, 0.05

granitic material (Barbey et al. 1989). The REE distributions show that transformation of metabasite into margin does not induce important modifications of REE. The global REE content (REE in Fig. 7) is unmodified [84-24, 89-57(1), 87-7], slightly increased [89-58, U10, 89-57(2), 87-5] or slightly decreased (89-75A'). The La/Yb and Eu/Eu* ratios (not represented) do not show large nor systematic variations. Figure 8 illustrates a most frequent situation: when the REE content is modified, its value in the margin is intermediate between that of metabasite and gneiss, suggesting a mixing. This hypothesis is supported by the observation that part of Z2 (this concerns especially zircon) is formed at the expense of the gneiss. Moreover, in a Zr versus REE diagram (Fig. 9), margins of samples 89-57(1), 89-57(2), 89-58 and 89-75A' have Zr and REE contents intermediate between those of their respective metabasite and gneiss whereas in margins 87-7 and 87-5, the REE and Zr contents is almost unmodified compared to that of the metabasite, suggesting that in these cases the gneiss immediately adjacent to the metabasite does not contain much zircon or apatite. Slight variations of REE have also been mentioned in the transition from amphibolite to granulite facies (Allen et al. 1985; Condie and Allen 1984; Weaver and Tarney 1983) but more important changes of REE have been reported by Stähle et al. (1987) during charnockitization in Kabbaldurga Quarry (South India) where zircon and apatite are progressively dissolved.

Comments

The behavior of major elements easily can be correlated with the mineralogical changes induced by the metasomatic process. The decrease in CaO is likely due to the disappearance of hornblende and, when it occurs, to the decrease in anorthite content of plagioclase. The depletion in Mg similarly can be explained by the increase in pyroxene Fe numbers. The replacement of hornblende (ca. 40% SiO_2: Table 3) by orthopyroxene (ca. 50% SiO_2) and, to a minor extent, the decreasing anorthite content in plagioclase can, together, account for the increase in SiO_2. The disappearance of biotite is responsible for K depletion. On the other hand, the perfectly inert status of Al_2O_3 is likely to be induced by the stability of plagioclase in the whole process. The X_{Mn} and MnO content of pyroxenes (cpx and opx) being almost constant when passing from the metabasite to the gneiss, the large increase in Mn is likely due to the increase in pyroxene proportion and/or to a higher Mn content in ilmenite. The source of this Mn is probably the metabasite itself but a thicker volume than the margin has been involved to yield the necessary Mn: mineral data have already shown that the diffusion process affecting Fe and Mg in pyroxenes was probably effective beyond the margin limits (see Fig. 4B).

Both Nb and Ta display the same feature as Mn but in this case metabasite and gneiss have a similar content of these elements. Minerals able to incorporate these ele-

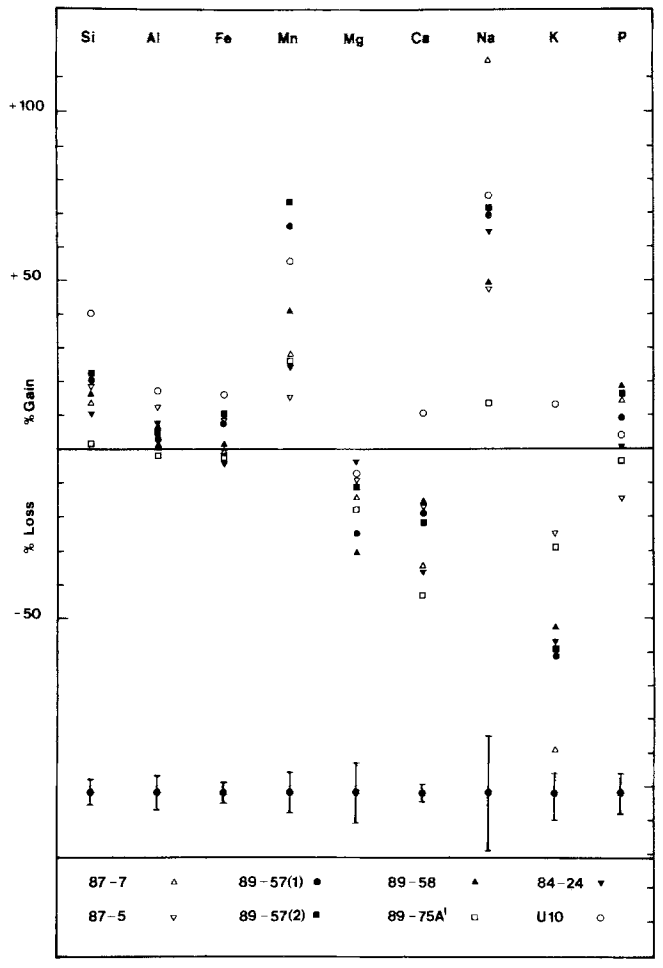

Fig. 6. Mass transfer evaluation for major elements with TiO_2 as a fixed component. Gains and losses are expressed as percentages relative to the protolith (metabasite). Error bars (average 2σ) calculated following the principle of error propagation (see Table 6)

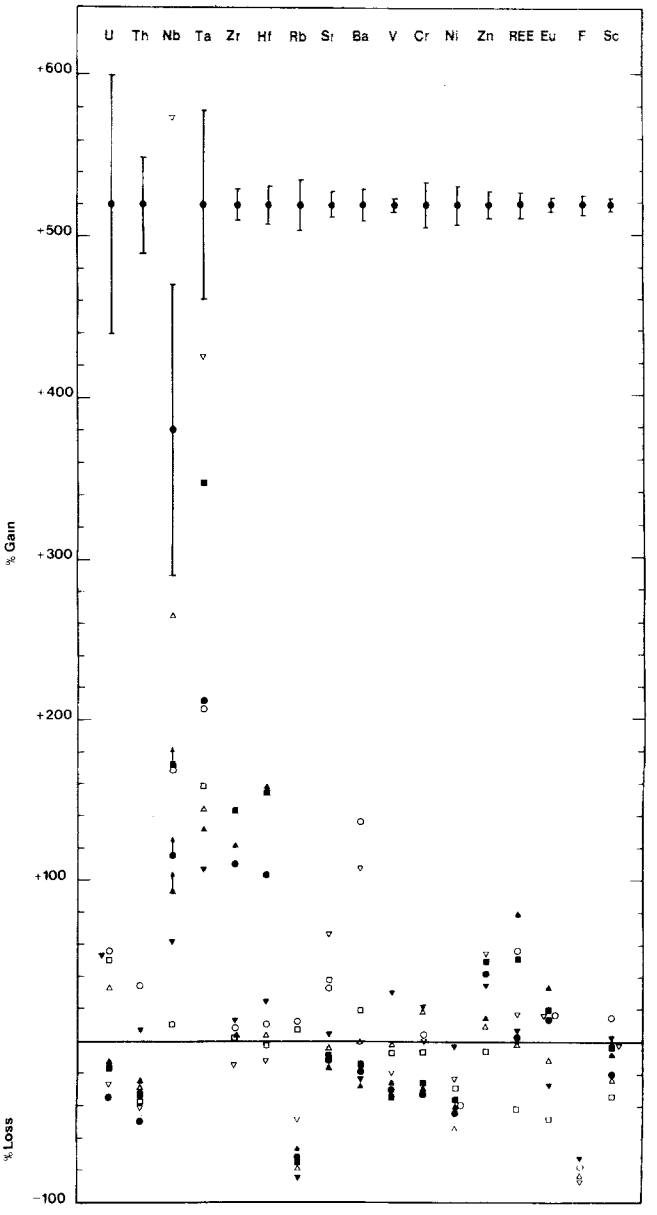

Fig. 7. Mass transfer evaluation for trace elements with TiO_2 as a fixed component. All errors are expressed as 1σ (see Table 6). Same symbols as in Fig. 6. Symbol with an *arrow* indicates a minimum value

ments in the margins are essentially ilmenite (Gottfried et al. 1968; Crecraft et al. 1981) and secondary biotite (Fourcade and Allègre 1981). Here again the source of Nb and Ta involves a larger part of probably both metabasite and gneiss than the volume of the margins.

The slight changes observed in V, Cr, Ni, and Zn can be explained by the stability of magnetite in the margins. The increase in Sr and Ba in U10 is probably due to the incorporation of K-feldspar from the gneiss. The same feature is observed in 87-5.

Disappearance of primary biotite in the reaction margin can account for Rb depletion, as formerly proposed by Rudnick et al. (1985) for low K granulites. According to microprobe data, the F-bearing phases are hornblende and biotite as well as apatite and the strong decrease of this element is due to the reaction of hydrated phases. In the margin, the remaining F is located in apatite (Roelandts et al. 1987). The strong depletion of F, H_2O, and K_2O as well as Rb from metabasite to zone Z1 is not balanced by reactions consuming these elements at the Z1/Z2 front or the Z2/gneiss front (no F-, H_2O- or K_2O-bearing phases are stable in the margins). This observation is not in agreement with Fisher's model (1973 – see "Origin of the margins" below) in which the growth of one diffusion zone is accomplished by an exchange cycle in which components evolved by reactions at one contact of a zone are consumed by reaction at the opposite contact (Joesten 1977, 1991 – see "Origin of the margins" below). It also implies that these components have been transported out of the system defined by the margins. To corroborate this conclusion, it is worth noting that a K-feldspar rich zone has been observed in the gneiss immediately adjacent to the margin of sample 89-57 (see petrographic section). On the other hand, H_2O could have induced a very small amount of partial melting in the adjacent gneiss as already suggested by petrographic data. Late biotite crystallized around oxides present in the margins during the M3 phase (retrograde metamorphism),

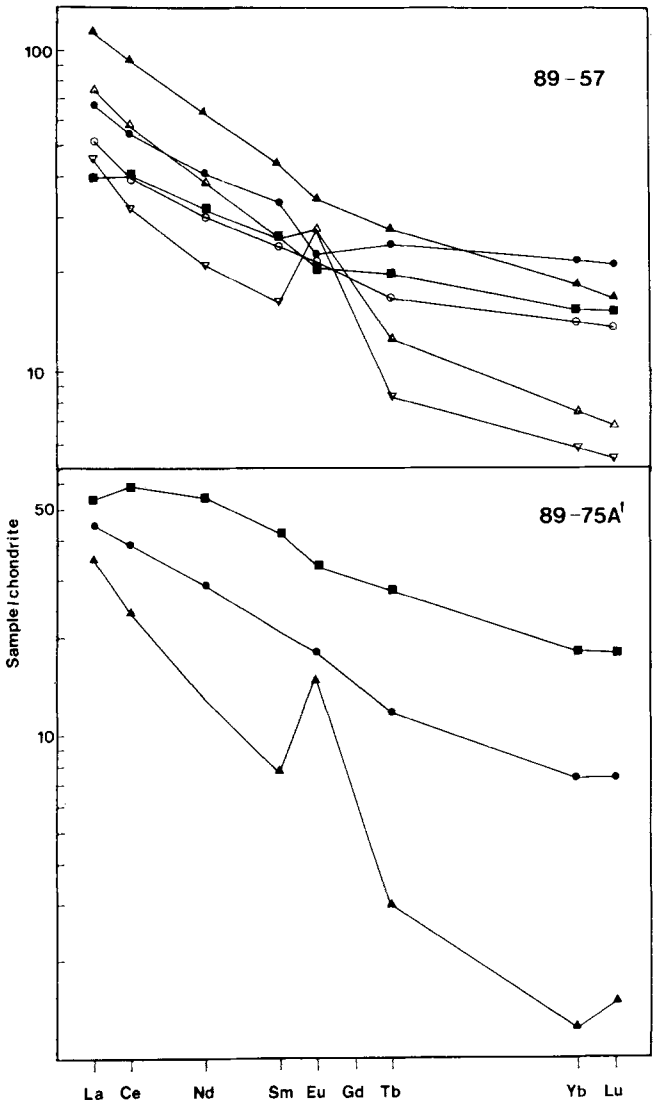

Fig. 8. Selected REE patterns of metabasite and corresponding margins and gneisses in two samples 89-57 and 89-75A'. Data are normalized with the values of Laul and Gosselin (1989). For each sample: ■, metabasite; ●, margin; ▲, gneiss. For sample 89-57: ■, metabasite; ●, margin (2); ▲, gneiss adjacent to the margin (2); ○, margin (1); △, gneiss adjacent to margin (1); ▽, K-feldspar-rich gneiss immediately adjacent to margin (1). Note that REE patterns of gneisses are variable

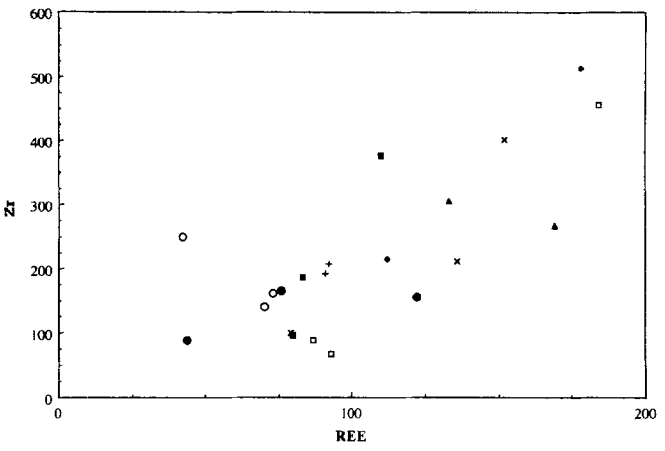

Fig. 9. Zr (ppm) versus ΣREE (ppm) for metabasites and corresponding margins and gneisses. □, 87-5; ○, 87-7; +, 84-24; ▲, U10; ●, 89-75A'; ×, 89-58; ◆, 89-57 (2); ■, 89-57 (1)

suggesting that H_2O and K_2O were still available in the rock at that time.

Origin of the margins

Introduction

In the mineral composition section, we have already shown that the zoned reaction margins were formed through a diffusion process. This observation implies that in the P–T conditions prevailing in this part of the granulite facies, the mineral assemblages of metabasite and gneiss are incompatible. The main goal of this section is to determine which chemical gradients control the diffusion process.

Korzhinskii's theoretical work (Korzhinskii 1970) on metasomatic zoning is based on two extreme types of metasomatism: diffusion and infiltration. In a diffusion process, the driving forces are the gradients in chemical potentials of some components between two contrasted rock types and elements are transported in the pore fluid. Due to the progressive evolution of chemical potentials, a succession of reactions occurs at different fronts (developing a typical metasomatic column) and solid solutions display a continuous chemical variation. In an infiltration process, different reactions also occur at different fronts and develop a metasomatic column due to reaction of the fluid with the rock. Depending on the shape of the curve in which concentration of component i in the fluid is a function of concentration of i in the solid (Hofmann 1972), solid solutions can display sharp differences at the interface between two zones. Diffusion and infiltration essentially differ due to the existence in diffusion metasomatism of a chemical equilibrium across each side of a sharp front, whereas in infiltration metasomatism there is disequilibrium across the front. In natural processes both types can theoretically combine and the predominance of one of them depends on the rock permeability, the existence of fluid pressure gradients and the flow rate of the percolating fluid relative to diffusion rates. Nevertheless, when infiltration occurs it generally dominates and the effects of diffusion are overprinted.

Diffusion processes have been described in many metamorphic environments: for example, replacement of one mineral by another (Johnson and Carlson 1990), or development of reaction zones between chemically incompatible beds (Vidale 1969; Thompson 1975; Brady 1977), this latter process being similar to the formation of the reaction margins discussed in this paper.

Fisher and Eliott (1974) showed that, in most metamorphic diffusion processes, the local equilibrium hypothesis (Thompson 1959) is verified and the process can be approximated by steady-state diffusion (Fisher 1973): zones grow by reactions at their contacts and the stoichiometry of these reactions is fixed by the relative diffusion fluxes within the zone. These fluxes take steady-state values that balance the rates of production and consumption of each component within the zone. Based on the local equilibrium hypothesis and the steady-state diffusion process, Joesten (1977) developed a model in which the different zone sequences that are stable in a steady-state process can be predicted. Moreover, the sequence of mineral zones, stable for a given choice of the relative values of the phenomenological coefficients for diffusion, can be obtained.

The approach followed in this paper is the graphical method proposed by Korzhinskii (1959) and Burt (1974) in which the saturation surface in chemical potential space allows the identification of the chemical potential gradients which are responsible for the observed succession of zones.

Several characteristics of the margins can be explained by the diffusion process:-

1. When an element becomes perfectly mobile, its μ is externally controlled and consequently, as the system gets one more degree of freedom, Korzhinskii's phase rule predicts that the number of phases is reduced by one. This takes into account the reduction of phase number in the margin compared to metabasite and gneiss;
2. Equations modeling the diffusion process (Korzhinskii 1970; Fonteilles 1978) show that the propagation speed of one front is inversely proportional to the distance it has moved and to the square root of time. Consequently, the speed decreases slowly with time and rapidly in space. It becomes negligible over a relatively small distance and the diffusion stops. This accounts for the small thickness of the diffusion reaction zones. On the other hand, the thickness is constant from samples to samples because similar reactions are involved.

Chemical potential diagrams in the system CaO-MgO-SiO_2-Al_2O_3-H_2O

The system CaO-MgO-SiO_2-Al_2O_3-H_2O. The major elements needed to describe the observed mineral assemblages are: SiO_2, Al_2O_3, MnO, FeO, MgO, CaO, Na_2O, K_2O, TiO_2, P_2O_5, H_2O. Using the status of components defined by Korzhinskii (1959), this system can be simplified in order to represent phase equilibria in chemical potential diagrams. Isocon diagrams (Fig. 5) have already shown that Al_2O_3, TiO_2, and P_2O_5 are perfectly inert components. As TiO_2 and P_2O_5 are present as major components only in ilmenite and apatite, respectively, they can be considered indifferent or accessory. The Mn occurs as a trace component replacing Fe and/or Mg in pyroxenes and does not induce the appearance of a new phase. When metabasites contain biotite, this mineral completely disappears in the margins (biotite mentioned in Table 2 belongs to M3 metamorphic phase) where no potassic phase is stable. This suggests that K_2O is a perfectly mobile component. Moreover, as margins are identical when metabasite contains biotite or is devoid of it, this component will not be considered in the system. The FeO is isomorphous with MgO and these two components will then be combined. The occurrence of margins both when there is a change and when there is not in the Mg no. [Mg/(Mg + Fe)] of pyroxenes supports this assumption. Moreover, isocon diagrams (Fig. 5) suggest that FeO and MgO are likely to be inert.

As already noted in the regional setting section, in the conditions of the granulite facies prevailing in the area, the hornblende + quartz assemblage reacts into pyroxenes at a lower temperature than the hornblende alone (the same holds for biotite). The reaction occurring at the metabasite/Z1 front is obviously similar but since quartz is not present in the metabasite, SiO_2 is supplied by diffusion: μ_{SiO_2} progressively must decrease through the margins from gneiss to metabasite since free quartz is present in the former ($a_{SiO_2} = 1$) and absent in the later ($a_{SiO_2} < 1$). As μ_{SiO_2} is fixed in any point of the margin by the diffusion process and the μ_{SiO_2} gradient is obviously controlling the occurrence of the margins, SiO_2 will be considered a perfectly mobile component. In Fig. 6 and in isocon diagrams (Fig. 5), Na_2O displays the strongest increase among major elements and we will then assume that this component is also perfectly mobile.

The status of H_2O is ambiguous. If margins develop in fluid present conditions (metamorphic fluid dominated by the system H-C-O), H_2O is an excess component. On the other hand, if the process occurs in fluid absent conditions (Thompson 1983), H_2O is most likely a perfectly mobile component. The occurrence of fluid present or fluid absent conditions is part of the debate concerning the reduced water activity prevailing during granulite formation. Nevertheless, in the P–T conditions of Rogaland, most rocks are likely to have low permeabilities and porosities suggesting that the metamorphic fluid (if present) is internally buffered with the possible existence of a_{H_2O} gradients (Waters 1988). Consequently, a perfectly mobile status will be considered for H_2O.

The initial system is then simplified to SiO_2-Al_2O_3-MgO-CaO-Na_2O-H_2O in which CaO and Na_2O cannot be treated together as CaO is present in cpx with no solid solution of Na_2O. Nevertheless, the solid solution of plagioclase will not be taken into account explicitly in the chemical potential diagrams but its influence on margin mineralogy will be discussed. This approximation is supported by the occurrence of margins even when there is no contrast in plagioclase composition between adjacent rocks. Following the above assumptions, the system is then reduced to: CaO-MgO-Al_2O_3-SiO_2-H_2O with plagioclase, quartz, orthopyroxene, clinopyroxene and hornblende.

The chemical potential diagrams. Three-dimensional chemical potential diagrams have been constructed using the crystallographic projection proposed by Grant (1977). Projection has been done from plagioclase as this mineral is stable in margins, gneiss and metabasite (Grant 1976).

Two diagrams have been considered in the simplified chemical system (CaO-MgO-SiO_2-Al_2O_3-H_2O) (Fig. 10A, B). In Fig. 10A with the μ_{H_2O}-μ_{MgO}-μ_{SiO_2} axes, the representative point of metabasite (M) is located at the intersection of the opx-cpx-hornblende saturation surfaces. The other end member of the diffusion column (gneiss) which should be located at the intersection of the opx-cpx-quartz saturation surfaces, cannot be shown. This diagram thus is not appropriate to represent the succession of zones observed in the margins. Nevertheless, it shows that the destabilization of hornblende could respond to a decrease of μ_{H_2O}. However, the μ_{H_2O} gradient which is likely to exist between metabasite and gneiss (Powell 1983) does not seem to have controlled the margin development as the different successions of zones cannot be obtained on this diagram.

On the other hand, in a μ_{SiO_2}-μ_{CaO}-μ_{MgO} diagram (Fig. 10B), the representative points of metabasite and gneiss can be shown and the succession of zones occurring in the three different types of margins (numbers 1, 2, 3 on Fig. 10B) are obtained along an increase of μ_{SiO_2} from metabasite to gneiss. This implies that the μ_{SiO_2} gradient is the main factor controlling the margin development. Moreover, in the first and third types of margin, when a value of μ_{SiO_2} is chosen, there is still one more degree of freedom, the value of μ_{CaO} or μ_{MgO}, i.e., one of these elements is perfectly mobile and the other one inert. The isocon diagrams suggest that MgO is likely to be the inert one. On the other hand, in the second type of margins, when the value of μ_{SiO_2} is chosen, μ_{MgO} and μ_{CaO} are also defined, i.e.,

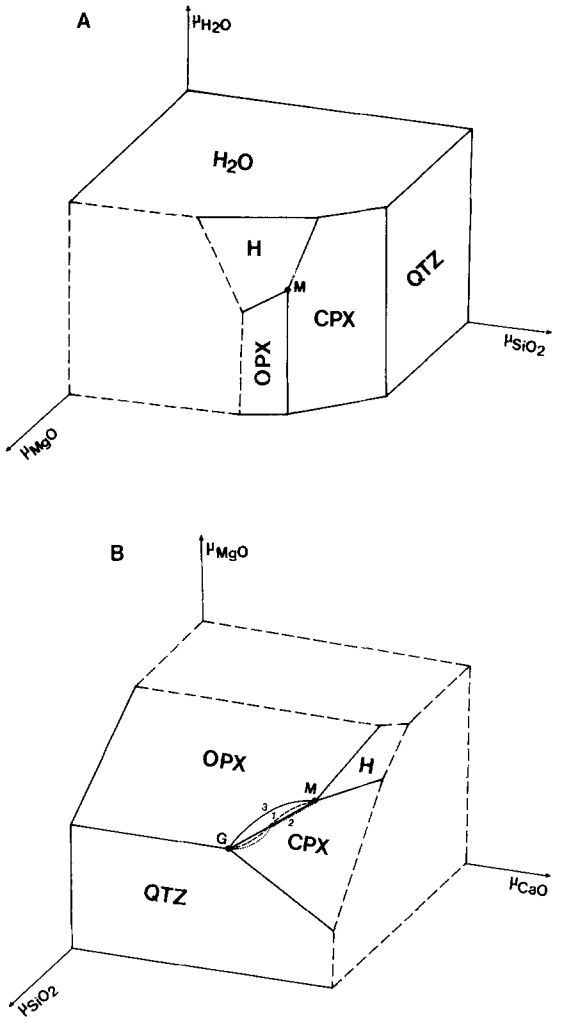

Fig. 10. Chemical potential diagrams in the system CaO-SiO_2-Al_2O_3-H_2O-MgO (Grant 1977) : **A, B** Projection has been done from plagioclase which is stable everywhere (Grant 1976). *H*, hornblende; *Opx*, orthopyroxene; *Cpx*, clinopyroxene; *M*, metabasite; *G*, gneiss. **B** The paths 1,2,3 display the succession of zones observed in the three types of margins (see text)

both μ_{CaO} and μ_{MgO} are controlled by the paragenesis and the two components are inert. This is in agreement with Korzhinskii's phase rule which predicts that the maximum number of phases equals the number of inert components. As zone Z1 of the second type of margins differs from that of the first and third types by the presence of cpx, the number of inert components must be increased by one unit (CaO). This 3D diagram suggests then that the behavior of CaO controls the variability of margin mineralogy. This different behavior of CaO is correlated with the composition of plagioclase. When plagioclase has a contrasted composition between adjacent rocks and the solid solution composition evolves continuously from the composition observed in the metabasite to that observed in the gneiss (Fig. 4A: first type of margin), CaO is perfectly mobile and cpx is unstable in zone Z1. When there is no difference in plagioclase composition between metabasite and gneiss (Fig. 4C: second type of margin), CaO is inert and cpx is stable in Z1.

The instability of cpx in zone Z1 of the first type of margin can be explained by reaction of this mineral with the Al_2O_3 evolved when plagioclase becomes more albitic. The following reactions can be written:

$$\text{Anorthite} + 1/2Na_2O + SiO_2 = 1/2Al_2O_3 + \text{albite} + CaO \quad (1)$$

$$\text{Cpx} + 1/2Al_2O_3 = 1/2\text{anorthite} + \text{opx} + 1/2CaO \quad (2)$$

with SiO_2 and Na_2O supplied by diffusion from the gneiss as shown by mass balance. As Al_2O_3 is a perfectly inert component, the Al_2O_3 produced by reaction (1) is consummed by reaction (2).

Petrographic data have shown that Z2 grew at the expense of both gneiss and Z1 and the reaction is likely to be

$$\text{Opx} + CaO + SiO_2 = \text{cpx} \quad (3)$$

In the third type of margin, no zone Z2 is observed: cpx occurs only as thin rims around some opx grains suggesting reaction (3). In the gneiss, pyroxenes are very scarce and K-feldspar occurs only as antiperthites in the plagioclase. One reactant of reaction (3) is thus missing inhibiting the development of zone Z2. This suggests that cpx is more efficiently produced from the gneiss than from Z1 (the a_{SiO_2} is higher in the gneiss). This explains the observation that the cpx grain size in Z2 is similar to that of the gneiss and considerably larger than that of the metabasite and implies in turn that the Z1/Z2 boundary could correspond to the original interface between metabasite and gneiss.

In Ollestadfjelli, petrographic data have shown that the margins developed when the intrusion was already crystallized, though the temperature at the liquidus stage was probably sufficiently high to induce the reaction. This feature could be due to the absence of a gradient in a_{SiO_2} between the inclusion and the surrounding magma and its subsequent appearance in the solid stage when quartz ($a_{SiO_2} = 1$) has crystallized.

Conclusions

The three different types of anhydrous pyroxene-bearing margins occurring at the contact between silica undersaturated metabasites and charnockitic gneisses in the granulite facies of Rogaland post-date any deformation and were formed through a diffusion process induced by the μ_{SiO_2} gradient existing between the adjacent rocks. Dehydration of the metabasite results from reaction between the diffusing SiO_2 and hornblende to form pyroxenes: this suggests that a μ_{H_2O} gradient is not prerequisite. As shown by chemical potential diagrams, the presence/absence of plagioclase with contrasting composition in adjacent rocks, which is correlated to the variable status of CaO (perfectly mobile or inert), determines the occurrence or non occurrence of cpx in Z1. Petrographic data and metasomatic reactions also suggest that the Z1/Z2 boundary corresponds to the original metabasite/gneiss interface. Moreover, the model proposed for the origin of these margins demonstrates that granulite facies parageneses can be obtained without the involvement of a partial melting process or a_{H_2O} gradients.

In this small-scale granulite formation, element mobilities are controlled by metasomatic reactions; relative to metabasite, no significant LILE depletion is observed, except for K and Rb due to the destabilization of biotite in the margins. Concentrations of Nb, Ta and Mn display the strongest increase. As no hydrous and potassic phases are stable in the margins, F, H_2O, K, and Rb produced by reactions of amphibole and biotite to form pyroxenes have been transported out of the system defined by the margins. This H_2O does not seem to have induced important partial melting in the adjacent gneiss as no coarse-grained, unfoliated parts have been observed in these gneisses. Nevertheless, the crystallization of late biotite around oxides during the M3 retrograde metamorphic phase suggests that H_2O and K_2O were still available in the system at that time.

Acknowledgments. The author is grateful to JC Duchesne (ULG, Belgium) who initiated this study, provided part of the samples as well as some geochemical data and supervised field work. J. Hertogen (KUL, Belgium), E. Wilmart and J.L. Joron (Lab. Pierre Süe, CEA – Saclay, France) are greatly thanked for providing NAA analyses as well as I Roelandts (ULG, Belgium) who made F determinations. XRF analyses were performed by G Bologne at the "Centre Interinstitutionnel de Géochimie Instrumentale" (Dir. J.C. Duchesne, ULG). G. Delhaze and V. Miocque also provided much help. We particularly thank J.C. Duchesne and M. Fonteilles (Université Paris VI, France) for their continuing support and useful comments. Constructive review from D.J. Waters contributed much and some of his suggestions have been incorporated. This research was supported by the Belgian Fund for Basic Research and the CGRI of the French Community of Belgium.

References

Allen P, Condie KC, Narayana BL (1985) The geochemistry of prograde and retrograde charnockite-gneiss reactions in Southern India. Geochim Cosmochim Acta 49:323–336

Barbey P, Cuney M (1982) K, Rb, Sr, Ba, U and Th geochemistry of the Lapland granulites (Fennoscandia): LILE fractionation controlling factors. Contrib Mineral Petrol 81:304–316

Barbey P, Bertrand JM, Angoua S, Dautel D (1989) Petrology and U/Pb geochronology of the Telohat migmatites, Aleksod, Central Hoggar, Algeria. Contrib Mineral Petrol 101:207–219

Bingen B (1989) Geochemistry of Sveconorwegian augen gneisses from SW Norway at the amphibolite-granulite-facies transition. Nor Geol Tidsskr 69:177–189

Bingen B, Demaiffe D, Hertogen J (1990) Evolution of feldspars at the amphibolite-granulite facies transition in augen gneisses (SW Norway): geochemistry and Sr isotopes. Contrib Mineral Petrol 105:275–288

Bohlen SR, Boettcher AL (1981) Experimental investigations and geological applications of orthopyroxene geobarometry. Am Mineral 66:951–964

Brady JB (1977) Metasomatic zones in metamorphic rocks. Geochim Cosmochim Acta 41:113–125

Burt DM (1974) Metasomatic zoning in Ca-Fe-Si exoskarns. In: Hofman AW, Giletti BJ, Yoder HS Jr, Yund RA (eds) Geochemical transport and kinetics. Carnegie Inst Washington Publ 634, pp 287–293

Condie KC, Allen P (1984) Origin of Archaean charnockites from Southern India. In: Kröner A, Hanson GN, Goodwin AM (eds) Archaean geochemistry. Springer, Berlin, Heidelberg New York, pp 182–203

Crecraft HR, Nash WP, Evans SH (1981) Late Cenozoic volcanism at Twin Peaks, Utah: geology and petrology. J Geophys Res 86-B11:10303–10320

Duchesne JC (1970) Microtextures of Fe-Ti oxide minerals in the South-Rogaland anorthositic complex (Norway). Ann Soc Geol Belg 93:527–544

Duchesne JC, Maquil R (1987) The Egersund-Ogna massif. In: Maijer C, Padget P (eds) The Geology of southernmost Norway: an excursion guide. Nor Geol Unders Spec Publ 1, pp 59–63

Duchesne JC, Michot J (1987) The Rogaland intrusive masses. In: Maijer C, Padget P (eds) The Geology of southernmost Norway: an excursion guide. Nor Geol Unders, Spec Publ 1, pp 59–63

Duchesne JC, Demaiffe D, Wilmart E (1987) Fidsel-Vardefjell-Itland: Apophysis, Hidra massif and envelope. In: Maijer C, Padget P (eds) The Geology of southernmost Norway: an excursion guide. Nor Geol Unders Spec Publ 1, pp 42–47

Falkum T, Petersen JS (1980) The Sveconorwegian Orogenic Belt, a case of Late-Proterozoic plate-collision. Geol Rundsch 69:622–647

Fisher GW (1973) Nonequilibrium thermodynamics as a model for diffusion-controlled metamorphic processes. Am J Sci 273:897–924

Fisher GW, Elliott DC (1974) Criteria for quasi-steady diffusion and local equilibrium in metamorphism. In: Hofman AW, Giletti BJ, Yoder HS, Yund RA (eds) Geochemical transport and kinetics. Carnegie Inst Washington Publ 634, pp 231–241

Fonteilles M (1978) Les mécanismes de la métasomatose. Bull Mineral 101:166–194

Fourcade S, Allègre CJ (1981) Trace element behaviour in granite genesis; a case study: the calc-alkaline association from the Quérigut Complex (Pyrénées, France). Contrib Mineral Petrol 76:177–195

Franssen L (1975) Etude comparative de l'orientation préférentielle des minéraux et leurs structures dans les gneiss catazonaux du Rogaland méridional (unpublished). Doctorat thèse, Univ Libre de Bruxelles

Gottfried D, Greenfield LP, Campbell EY (1968) Variation in Nb-Ta, Zr-Hf, Th-U, K in diabase – granophyre suites. Geochim Cosmochim Acta 32:925–947

Grant JA (1976) Mineral assemblages in stereographic projection. Am Mineral 61:1020–1024

Grant JA (1977) Crystallographic projection of chemical potential relationships as an aid in the interpretation of metasomatic zoning. Am Mineral 62:1012–1017

Grant JA (1986) The isocon diagram – a simple solution to Gresens' equation for metasomatic alteration. Econ Geol 81:1976–1982

Gresens RL (1967) Composition-volume relationships of metasomatism. Chem Geol 2:47–65

Heier KS, Thorensen K (1971) Geochemistry of high-grade metamorphic rocks, Lofoten-Westeralen, North Norway. Geochim Cosmochim Acta 35:89–99

Hermans GAEM, Tobi AC, Poorter RPE, Maijer C (1975) The high-grade metamorphic Precambrian of the Sirdal-Orsdal area. Nor Geol Unders 318:51–74

Hofmann AW (1972) Chromatographic theory of infiltration metasomatism and its application to feldspars. Am J Sci 272:69–90

Iyer SS, Choudhuri A, Vasconcellos MBA, Cordani UG (1984) Radioactive element distribution in the Archean granulite terrane of Jequia, Bahia, Brazil. Contrib Mineral Petrol 85:95–101

Jansen B, Blok R, Bos A, Scheelings M (1985) Geothermometry and geobarometry in Rogaland and preliminary results from the Bamble area, south Norway. In: Tobi A, Touret JLR (eds) The deep Proterozoic crust in the North Atlantic Provinces (NATO Adv Sci Inst Ser C 158). Reidel, Dordrecht, pp 499–518

Joesten R (1977) Evolution of mineral assemblage zoning in diffusion metasomatism. Geochim Cosmochim Acta 41:649–670

Joesten R (1991) Local equilibrium in metasomatic processes revisited: diffusion-controlled growth of chert nodule reaction rims in dolomite. Am Mineral 76:743–755

Johnson CD, Carlson WD (1990) The origin of olivine-plagioclase coronas in metagabbros from the Adirondack Mountains, New York. J Metamorphic Geol 8:697–717

Katz MB (1969) The nature and origin of the granulites of Mont Tremblant, Quebec. Bull Geol Soc Am 80:2019–2038

Korzhinskii DS (1959) Physicochemical basis of the analysis of the paragenesis of minerals. New York Consultants Bureau

Korzhinskii DS (1970) The theory of metasomatic zoning. Clarendon Press, Oxford

Lambert IB, Heier KS (1967) The vertical distribution of uranium, thorium, and potassium in the continental crust. Geochim Cosmochim Acta 32:377–390

Laul JC, Gosselin DC (1989) Radioanalytical methods for rare earth elements in geological and biological materials. In: Bünzli JCG, Choppin GR (eds) Lanthanide probes in life, chemical and earth sciences. Elsevier, Amsterdam, pp 351–389

Maijer C (1987) The metamorphic envelope of the Rogaland intrusive complex. In: Maijer C, Padget P (eds) The Geology of southernmost Norway: an excursion guide. Nor Geol Unders, Spec Publ 1, pp 121–133

Maijer C, Andriessen P, Hebeda E, Jansen J, Verschuren R (1981) Osumilite, an approximately 970 Ma old high temperature index mineral of the granulite-facies metamorphism in Rogaland, SW Norway. Geol Mijnbouw 60:267–272

Powell R (1983) Processes in granulite facies metamorphism. In: Atherton MP, Gribble CD (eds) Migmatites, melting and metamorphism. Shiva Geology Series, Nantwich, pp 127–139

Priem HNA, Verschure RH (1982) Review of the isotope geochronology of the high-grade metamorphic Precambrian of SW Norway. Geol Rundsch 71:81–84

Ramberg H (1948) Titanium iron ores formed by dissociation of silicates in granulite facies. Econ Geol 43:553–570

Roelandts I, Robaye G, Weber G, Delbrouck JM, Duchesne JC (1987) Determination of fluorine by proton induced gamma ray emission (PIGE) spectrometry in igneous and metamorphic charnockitic rocks from Rogaland (SW Norway). J Radioanal Nucl Chem 112:453–460

Rudnick RL, McLennan SM, Taylor SR (1985) LILE in rocks from high-*P* granulite facies terrains. Geochim Cosmochim Acta 49:1645–1655

Schrijver K (1973) Bimetasomatic plagioclase-pyroxene reaction zones in granulite facies. Neues Jahrb Mineral Abh 119:1–19

Sighinolfi GP, Figueredo MCH, Fyfe WS, Kronberg BI, Tanner Oliveira MAF (1981) Geology and petrology of the Jequie granulitic complex (Brazil) : an Archean basement complex. Contrib Mineral Petrol 78:263–271

Stähle HJ, Raith M, Hoernes S, Delfs A (1987) Element mobility during incipient granulite formation at Kabbaldurga, Southern India. J Petrol 28(5) :803–834

Thompson AB (1975) Calcsilicate diffusion zones between marble and pelitic schist. J Petrol 16(2) :314–334

Thompson AB (1983) Fluid absent metamorphism. J Geol Soc London 140:533–547

Thompson JB (1959) Local equilibrium in metasomatic processes. In: PH Abelson (ed) Researches in Geochemistry. Wiley Interscience, Chichester New York, pp 427–457

Thompson JB (Jr) (1970) Geochemical reactions and open systems. Geochim Cosmochim Acta 34:529–551

Tobi AC, Hermans GAEM, Maijer C, Jansen JB (1985) Metamorphic zoning in the high-grade Proterozoic of Rogaland-Vest Agder, SW Norway. In: Tobi A, Touret JLR (eds) The deep Proterozoic crust in the North Atlantic Provinces (NATO Adv Sci Inst, Ser C 158). Reidel, Dordrecht, pp 477–497

Topping J (1966) Errors of observation and their treatment, 3rd edn. The Institute of Physics and the Physical Society (ed) Chapman and Hall, London

Versteeve AJ (1975) Isotope geochronology in the high-grade metamorphic Precambrian of Southwestern Norway. Nor Geol Unders 318:1–50

Vidale R (1969) Metasomatism in a chemical gradient and the formation of calcsilicate bands. Am J Sci 267:857–874

Waters DJ (1988) Partial melting and the formation of granulite facies assemblages in Namaqualand, South Africa. J Metamorphic Geol 6:387–404

Weaver BL, Tarney J (1983) Elemental depletion in Archean granulite facies rocks. In: Atherton MP, Gribble CD (eds) Migmatites melting and metamorphism. Shiva Geology Series, Nantwich, pp 250–263

Wielens JBW, Andriessen PAM, Boelrijk NAIM, Hebeda EH, Priem HNA, Verdurmen EAT, Verschure RH (1980) Isotope geochronology in the high-grade metamorphic Precambrian of Southwestern Norway: new data and reinterpretations. Nor Geol Unders 359:1–30

Wilmart E, Duchesne JC (1987) Geothermobarometry of igneous and metamorphic rocks around the Ana-Sira anorthosite massif: implications for the depth of emplacement of the South Norwegian anorthosites. Nor Geol Tidsskr 67:185–196

Wilmart E, Hertogen J, Roelandts I, Duchesne JC (1987) Geochemistry of Proterozoic supracrustals, granite-gneisses and charnockites from the envelope of the Ana-Sira anorthosite massif (Southwest Norway) (abstract). Colloq IGCP 217 Proterozoic Geochem, Lund

Editorial responsibility: W. Schreyer